FRP strengthened SHS beam-column connection under monotonic and large-deformation cyclic loading

T. Tafsirojjaman [a,b], Sabrina Fawzia [a,*], David P Thambiratnam [a], Xiao-Ling Zhao [c]

[a] School of Civil and Environmental Engineering, Faculty of Science and Engineering, Queensland University of Technology, 2 George Street, Brisbane, QLD 4000, Australia.

[b] Centre for Future Materials (CFM), School of Civil Engineering and Surveying, University of Southern Queensland, Toowoomba, QLD 4350, Australia.

[c] Department of Civil and Environmental Engineering, The University of New South Wales (UNSW), Sydney, NSW 2052, Australia.

([*]Corresponding author: sabrina.fawzia@qut.edu.au, Tel: 61731381012, Fax: 61 7 31381170

Email addresses: tafsirojjaman@hdr.qut.edu.au (T. Tafsirojjaman),

sabrina.fawzia@qut.edu.au (Sabrina Fawzia), d.thambiratnam@qut.edu.au (DP Thambiratnam), xiaolin.zhao@unsw.edu.au (Xiao-Ling Zhao)

ABSTRACT

Many civil applications use square hollow sections (SHSs) as members in beam-column connections which can be vulnerable under cyclic loading. Cyclic loadings from earthquakes, wind, waves and currents affect onshore and offshore civil infrastructure. In addition, these beam-column connections can become structurally inadequate through incremental service loads, design/fabrication errors and material property degradation over time. Due to this, it will be necessary to strengthen SHS beam-column connections to improve their performance under sustained monotonic and cyclic loadings. This paper treats the performance of SHS beam-column connections strengthened with externally bonded carbon fibre reinforced polymer

(CFRP) and glass fibre reinforced polymer (GFRP). Experimental investigations have been conducted on the bare, CFRP and GFRP strengthened SHS connections under monotonic and cyclic loading. Results show that under cyclic loading both CFRP and GFRP strengthened SHS beam-column connections exhibit improved ultimate moment capacity, moment degradation behaviour, secant stiffness, energy dissipation capacity and plastic hinge behaviour compared to their bare counterparts. Under monotonic loading, both types of strengthened connections show higher moment capacity, secant stiffness and ductility. In addition, CFRP strengthening enhances the ultimate strength, while GFRP strengthening enhances ductility.

Keywords: Square hollow sections (SHS) beam-column connections; Carbon fibre reinforced polymer (CFRP); Glass fibre reinforced polymer (GFRP); Strengthening; Monotonic loading; Cyclic loading.

1. Introduction

Beam-columns connections using square hollow sections (SHSs) as members in steel structures are quite common and used extensively due to their many structural and architectural advantages [1,2]. SHSs show better structural performance in comparison to other open sections in torsion, and compression, as well as offer more fire protection options and better capability to resist corrosion due to the absence of sharp edges [1]. SHSs are used in columns, beams, beam-column connections, lattice girders and facades of civil infrastructures.

Earthquakes have caused significant damage to structures and resulted in significant loss of human life. In the 20^{th} century alone, this natural disaster has resulted in 1.87 million casualties. A single earthquake has caused an average of 2052 deaths between 1990 and 2010 [3]. Recently, the frequency of earthquakes occurring globally has increased [4]. Cyclic loading is now an important concern as the major cause of structural failure has been through steel fractures in hollow members [5]. Seismic loading which is a kind of cyclic loading, can cause

structural connections to fail in isolation, causing failure in sections of a building or entire collapse of the structure [6]. This can occur either through horizontal acceleration or ground liquefaction [7]. The cyclic loading generated from earthquakes and winds affects both onshore and offshore structures. Offshore structures, mainly the oil and gas extraction support platform of the mining industry, face cyclic loading through current and waves in addition to earthquakes and winds [5]. Strong-column weak-beam is the main concept in the design of moment-resisting frames. Steel structures such as hospitals and other public facilities were damaged severely due to the Northridge earthquake in 1994. Both high-rise and low-rise buildings, and the old, as well as the new buildings were damaged. Damage in welded beam-column connections was the most common damage. Damage was found in 75% of the connections in the surveyed buildings. At least one connection was severely damaged in 70% of the floors and in several cases, all the connections were damaged in one or more floors of the building [8]. The columns had buckled and the flanges of girders had yielded and buckled as well in some steel structures [9]. In 1995 in the Hyogo-ken Nanbu earthquake, more severe damage was observed and the damage of steel-framed structures was due to failures of columns, column bases, beams and beam-column connections [10]. In addition to such random loading, SHS beam-column connections can also become structurally inadequate through incremental service loads, design/construction errors and material property degradation. Researchers aim to repair or strengthen these connections to improve their performance under sustained cyclic loading. However, studies on cyclic loading on SHS beam-column connection is limited.

Currently, the standard method of repairing and strengthening connections in steel structures is through welding extra steel plates where needed. This results in added weight and sometimes altered stress distributions due to the heat created during the welding [11]. These welded plates are also vulnerable to damage from corrosion [12]. This process often requires heavy machines, scaffolding and long disruptions to services during the repairs [5]. Strengthening or repairing

through fibre reinforced polymer (FRP) is increasing nowadays [13] and can circumvent these issues while providing additional benefits. These include higher tensile strength and strength to weight ratio [14,15], resistance to corrosion [16,17], cheaper as less preparation and labour are required, easy to apply in confined spaces, increased flexibility and the ability to form any shape [18]. Research has demonstrated the ability of FRP strengthening to improve the moment capacity and ductility of the steel members [2,19,20], enhance resistance to impacts [21] and reduction in tip displacement in rigid steel frames under lateral loads [22–24]. FRP strengthening can delay local buckling [25], increase steel member energy absorption capacity [26] and improve the fatigue behaviour of the steel members [27] and plates [28,29]. Moreover, FRP strengthening technique has been effective in enhancing the axial capacity of SHSs [30,31], lipped channel steel sections [32] and concrete-filled steel tubes [33]. Based on the above advantages of FRP, both carbon fibre reinforced polymer (CFRP) and glass fibre reinforced polymer (GFRP) strengthening techniques have been used to repair and strengthen SHS steel beam-column connections subjected to both monotonic and cyclic loading. Moreover, there are different beam-column connections e.g. welded, bolted, combined welded and bolted etc [34]. Welded beam-column connection is chosen in the present study as except for its fracture tendency index, it possesses good load carrying capacity, hysteretic behaviour and cumulative damage resistance under seismic and cyclic loadings [35] and the FRP strengthening technique will be effective to enhance its fracture resistance capacity.

Although there have been some investigations on FRP strengthening of welded connections under fatigue loading, e.g. welded steel attachments [36], welded cross-beam connections [37], welded web gusset joints [38], K-joints [39], the behaviours of FRP strengthened SHS beam-column connections under large-displacement cyclic and monotonic loadings have not yet been investigated. Hence, there is an urgent need to investigate the behaviour of FRP strengthened SHS beam-column connections subjected to monotonic and cyclic loading. In the present

study, the monotonic push loading and cyclic push-pull loading are applied with a hydraulic actuator at the beam tip to investigate the behaviour of FRP strengthened SHS beam-column connections under monotonic and cyclic loadings. Six SHS welded beam-column connections with the same column and beam sizes are prepared. Both CFRP and GFRP are used for the strengthening using the same adhesive in order to investigate the effect of FRP type. Structural performance in terms of moment capacity, secant stiffness, energy dissipation and ductility of the bare, CFRP and GFRP strengthened SHS beam-column connections under monotonic loading are compared first. This is followed by evaluating the effects of continued cycling on the behaviour of the bare, CFRP and GFRP strengthened SHS beam-column connections with respect to the same performance indicators. Moreover, the development of plastic hinge and the propagation of yielding along the beam length are investigated for all the SHS beam-column connections under cyclic loading.

2. Experimental Program

2.1 Materials

Four different materials namely, steel, adhesive, CFRP and GFRP were used in the present study. Liberty OneSteel Ltd., Australia supplied the cold-formed SHS steel sections. The grade of the steel was C350L and was manufactured according to AS/NZS 1163 [40]. The standard coupons of steel are prepared from the SHS steel sections and the mechanical properties of steel are obtained through standard coupon tests according to AS1391 [41]. Figure 1 shows the stress-strain curves obtained from the standard coupon tests. As there is no definite yield plateau, the yield stress is obtained using the 0.2% offset method. The measured average modulus of elasticity, yield stress and tensile strength were 190 GPa, 380 MPa and 475 MPa respectively. CF130 normal modulus, unidirectional and with nominal dry thickness of 0.176 mm are used as CFRP and supplied by BASF Pty Ltd., Australia. The used GFRP sheets were

manufactured and supplied by CG Composites Pty Ltd., Australia. Tensile tests of epoxy coated cured CFRP and GFRP sheets were undertaken by one of the authors according to ASTM: D3039 [42] to determine the sheet's mechanical properties. The measured average modulus of elasticity and tensile strength were 75 GPa and 987 MPa respectively for CFRP [43] and 55 GPa and 1065 MPa respectively for GFRP [44]. The thicknesses of CFRP and GFRP laminates are measured by using digital Vernier callipers in three different locations. The measured average thicknesses of one-layer CFRP and GFRP laminate are 0.60 mm and 0.65 mm respectively. MBrace 3500 and MBrace 4500 two-part epoxy resin manufactured and supplied by BASF construction chemicals Australia Pty Ltd. are used as adhesion promoter primer and bonding material respectively in the present study. Standard tensile coupon tests were conducted in accordance with ASTM: D638-10 [45] by one of the authors to measure the material properties of adhesive [46]. The average modulus of elasticity and tensile strength of adhesive were 2.86 GPa and 46 MPa respectively.

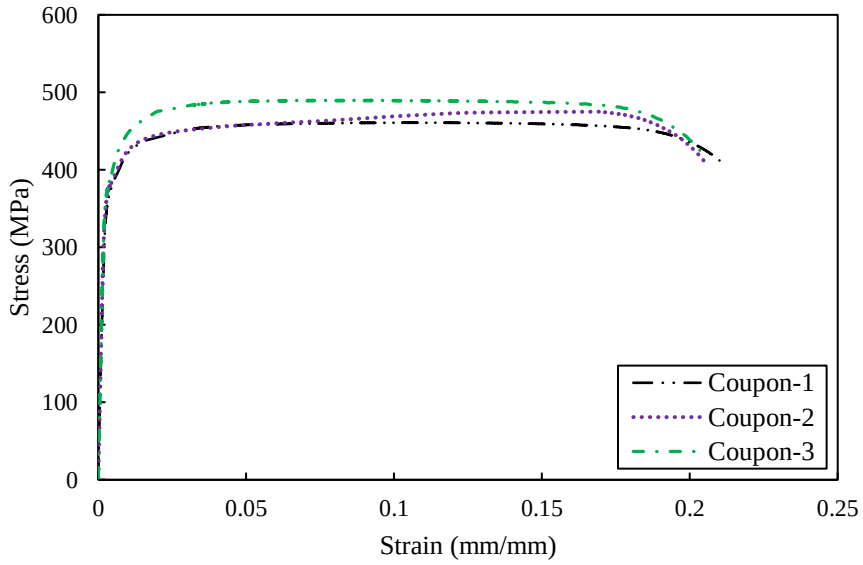

Figure 1: Stress–strain curves from the standard coupon tests.

2.2 Experimental specimens and schemes of strengthening

Six identical SHS welded beam-column connections are prepared. SHS 100×100×3 (mm) and 100×100×9 (mm) were used as beam and column respectively for all the specimens. The beam section was non-compact whereas the column section was compact. The SHS members were selected by considering the strong-column weak-beam concept. The beam is welded all around with the column by complete joint penetration (CJP) groove welds according to AWS D1.1 [47]. CJP groove weld was used to reduce the probability of welding failure. Steel end plates of 20 mm thickness are welded at both ends of the column and connected with the pin supported connections while the same endplate is welded at the tip end of the beam to be connected with the load transferring hinges.

For clarity in results, the specimens are labelled for identification. The first term is the type of connection - BBCC denotes the bare beam-column connections and SBCC denotes the FRP strengthened beam-column connections. The next text denotes the types of FRP used for strengthening where B stands for bare connections, C for CFRP strengthened connections and G for GFRP strengthened connections. The last letter denotes the applied loading condition during the experiment - M for monotonic loading and C for cyclic loading. Details are given in Table 1 for each specimen.

Table 1: Experimental specimens matrix

Specimen types	Specimen identifier	Types of FRP	Loading condition
Bare beam-column connection	BBCC-B-M	-	Monotonic
Strengthened beam-column connection	SBCC-C-M	CFRP	Monotonic
Strengthened beam-column connection	SBCC-G-M	GFRP	Monotonic
Bare beam-column connection	BBCC-B-C	-	Cyclic

Strengthened beam-column connection	SBCC-C-C	CFRP	Cyclic
Strengthened beam-column connection	SBCC-G-C	GFRP	Cyclic

The beams of all strengthened beam-column connections are strengthened with the same bond length of 300 mm FRP with the FRP fibre direction of LLH, which means that FRP fibres are in the longitudinal direction (L) in both first and second layers and in the hoop direction (H) in the third layer. The FRP fibre orientation of LLH is chosen to utilise the higher stiffness and tensile strength of FRP in the longitudinal direction in the first two layers and the third layer in the hoop direction to clip and confine the first two layers for better debonding resistance. The columns of all the beam-column connections are strengthened with the same bond length of FRP of 200 mm. The FRP fibre orientation of first and third layers is in the hoop direction to clip and confine the overlapped FRP from the beams while the second layer is in the longitudinal direction to utilise the advantages of FRP's longitudinal properties. The schematic diagram of the FRP strengthened connection is shown in Figure 2.

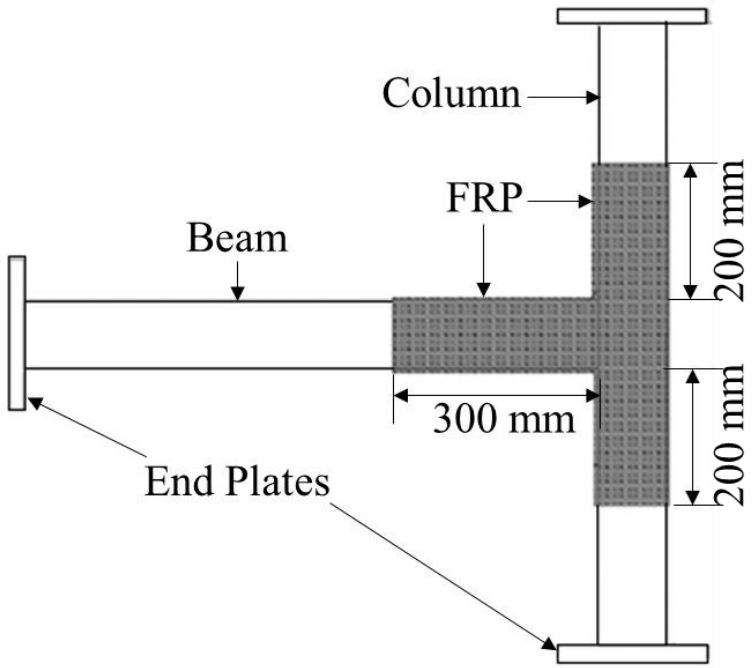

Figure 2: Schematic diagram of the FRP strengthened connection

2.3 Preparation of specimen and strengthening procedure

Two specimens remained untreated and left as bare steel connections to be used as control specimens for the monotonic and cyclic tests. The steel surface of SHS beam-column connections was roughened by sandblasting in the area to be strengthened to ensure a sound adhesion of the FRP with the steel surface and shown in Figure 3(a). Grease and any remaining particles were cleaned using acetone with a cloth. Once the acetone had dried, the area is primed with the adhesion promoter and left to sit for a minimum of 45 minutes and shown in Figure 3(b). The epoxy part A and B are then mixed thoroughly as a ratio of 1:3 and applied into the primed area as stated in the guidelines provided by the manufacturer. The FRP sheets are prepared according to the required dimensions and applied one layer at a time. The first layers are applied in the adhesive coated steel surfaces (around the top and bottom of the beam and front and back of the column) of the beam-column connection. The sheets are rib rolled in the direction of the main fibres to ensure full saturation of the fibres and with the adhesive coming through as shown in Figure 3(c). Before applying the second layer of FRP, the additional adhesive is applied on the first layer and rib rolled again in the direction of the main fibres. The third layer is then applied above the second layer by following the same procedure as before. This whole process was conducted while all layers remained saturated with epoxy to promote bonding between all layers and the bare steel section. Hence, after curing it will behave as a single laminate of FRP. Then the strengthened area is wrapped with masking tape to prevent premature debonding and shown in Figure 3(d). The masking tape was removed from the strengthened connection after 24 hours of curing. To confirm the achievement of proper bonding, the strengthened connections were cured for a minimum of two weeks in ambient

temperature. All tested bare, CFRP and GFRP strengthened beam-column connections are shown in Figure 4.

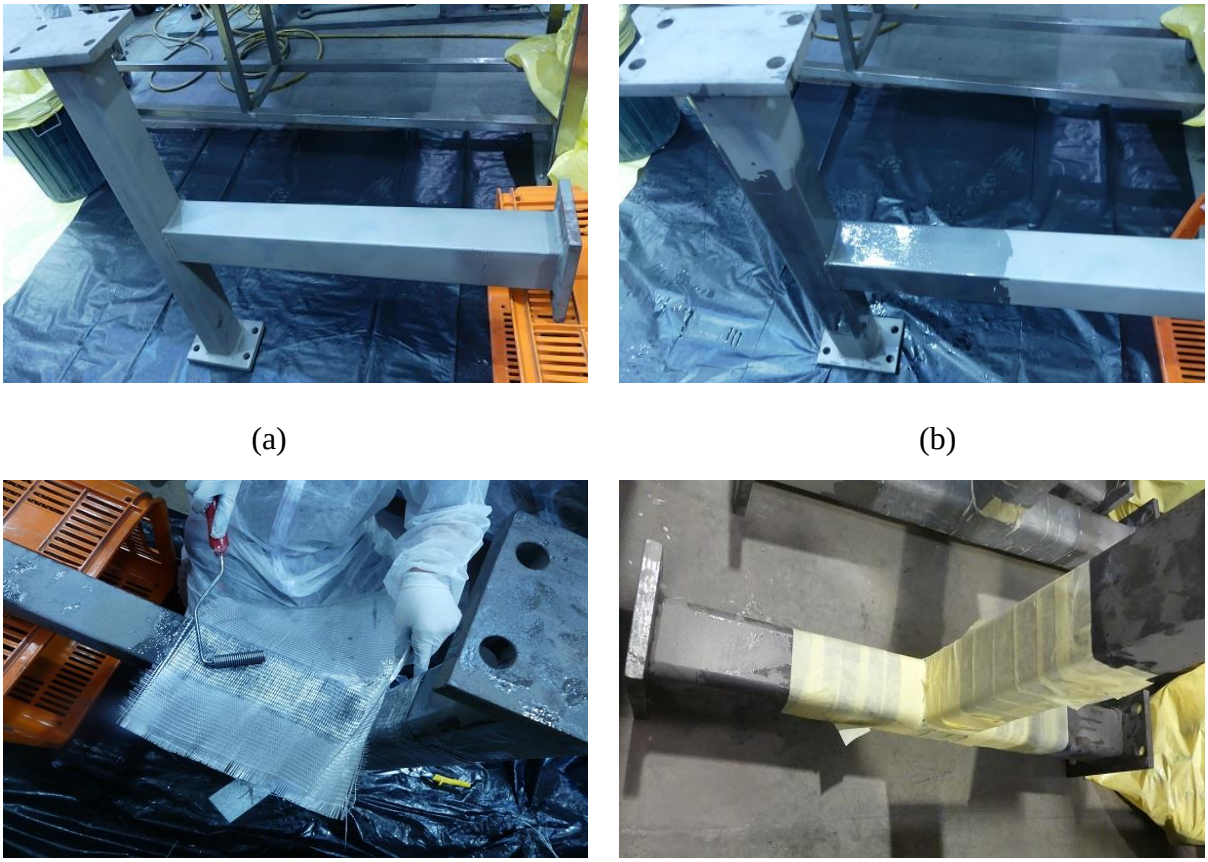

(a) (b)

(c) (d)

Figure 3: Specimen preparation: (a) specimen after sandblasting; (b) process of rib rolling; (c) application of masking tape (d) cured connection

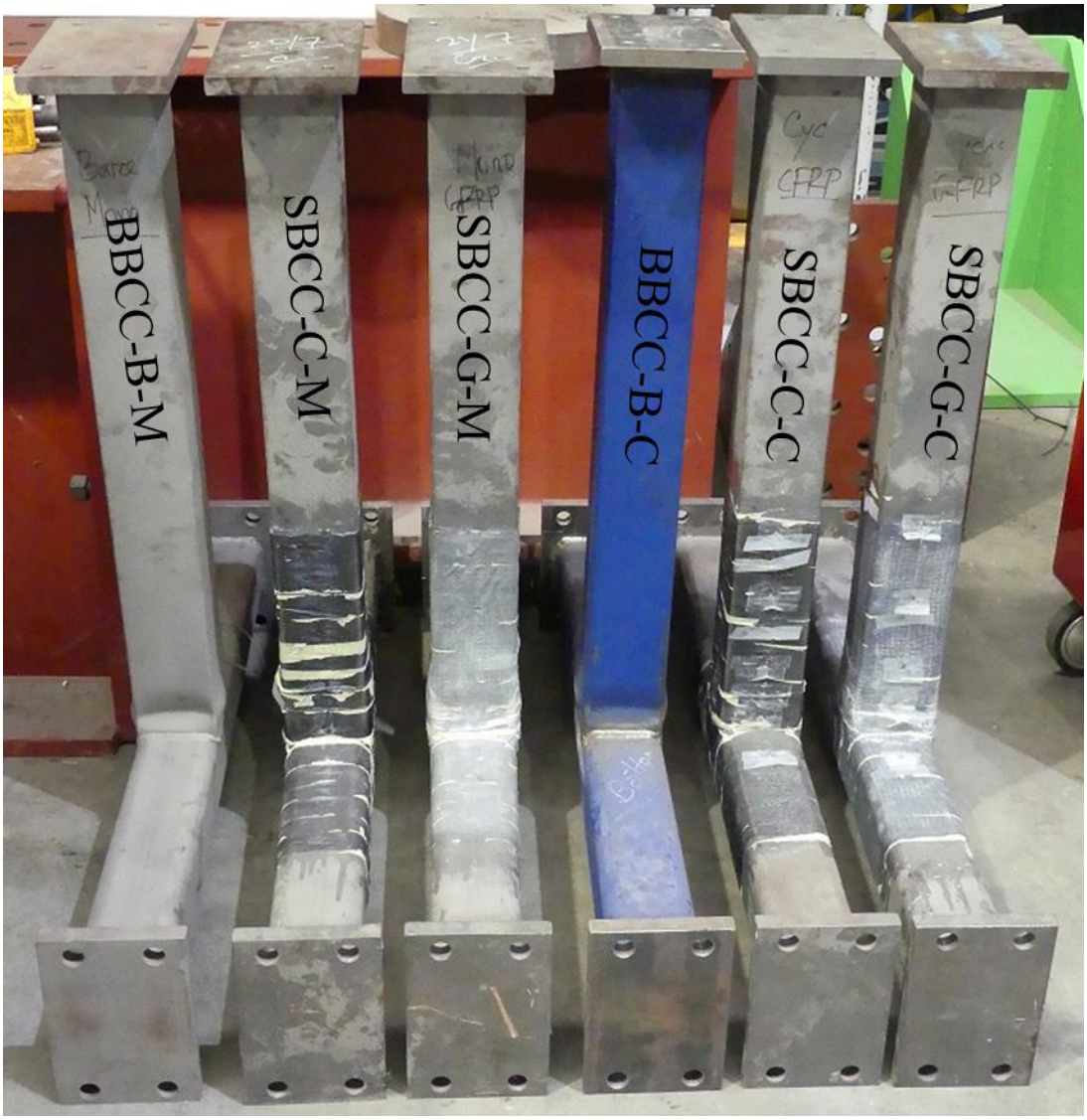

Figure 4: Tested bare, CFRP and GFRP strengthened SHS beam-column connections

2.4 Experimental setup and loading protocol

The exterior SHS beam-column connection in rigid moment frames is characterised by the tested SHS beam-column connections of the present study. The SHS was supported vertically at the top and bottom ends through pinned connections to represent the points of inflection at the column ends accurately. The SHS beam is horizontally cantilevered out perpendicular to the column face so that the tip of the SHS beam will be directly under the hydraulic loading point. The beam is connected to the hydraulic through a doubly pinned hinge to avoid any axial load and to investigate the connections under pure bending. A thick bearing plate is welded to

the tip of the beam and bolted to the pinned hinge connected to the hydraulic to avoid local deformations due to applied loading. This setup allows for vertical push loading required during the monotonic testing and both vertical push and pull loading required during the cyclic testing as well. A schematic diagram of the experimental setup is shown in Figure 5(a).

The used hydraulic actuator has a loading capacity of 1000 kN and the ability to measure applied displacements and loads. The applied load at the tip of the beam is multiplied by the lever arm (1000 mm) to determine the applied moment. The displacement at various sections of the specimen is measured using Laser Displacement Sensors (LDS). Strain gauges are placed at 50 mm, 100 mm, 200 mm and 300 mm from the column front face on the centre of the top face of the beam. Figure 5(b) shows a photograph of the experimental setup. The increasing displacement control large-deformation cyclic loading protocol as specified in ANSI/AISC 341-16 [48] was used for the cyclic loading tests and shown in Figure 6. This earthquake simulation protocol was selected as current provisions for earthquakes require the connections to undergo the large deformation and simulate far field type earthquakes [48]. The displacement at the end of the beam is divided by the lever arm of the loading point (1000 mm) to determine the rotation experienced by each connection according to ANSI/AISC 341-16 [48]. A small amount of flexibility was noticed at the supports of the connection and loading point during the testing of each specimen (Figure 5(b)).

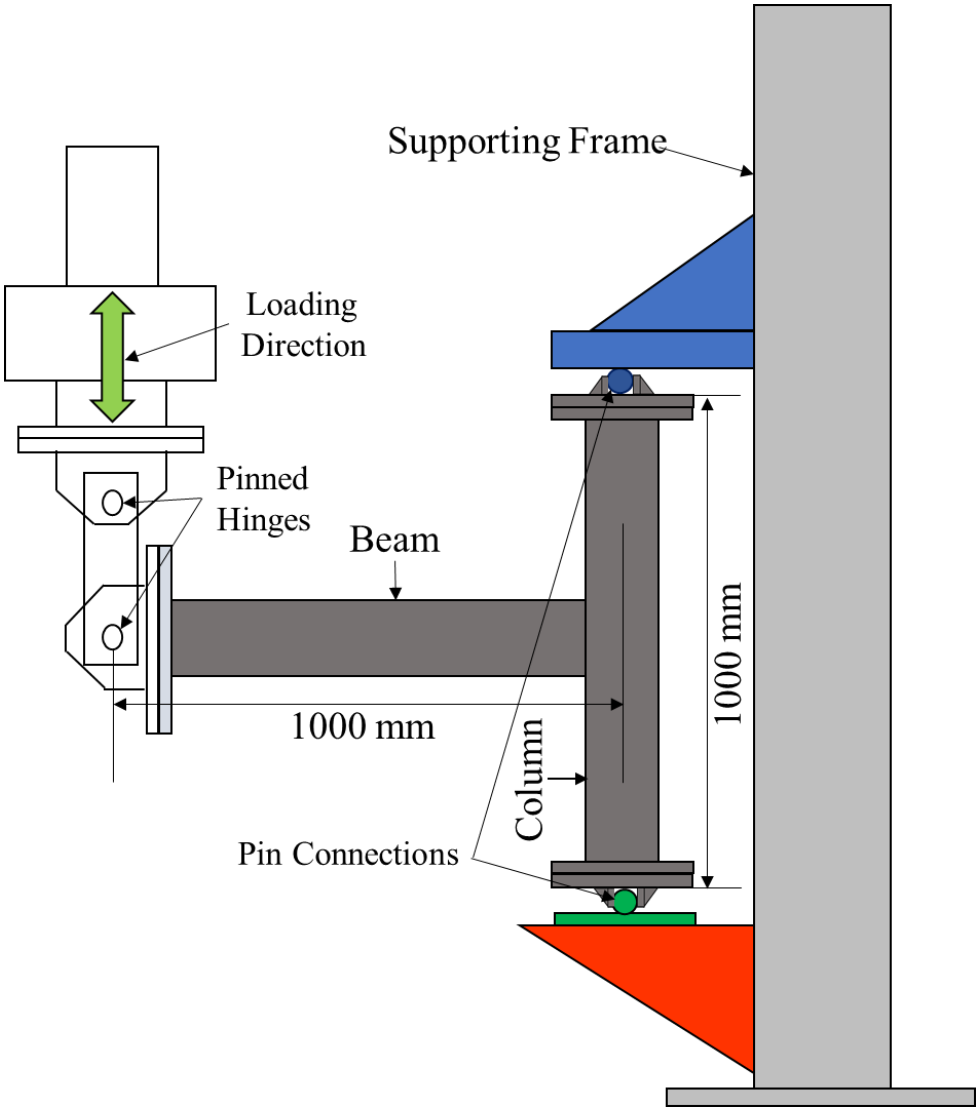
Supporting Frame
Loading
Direction
Pinned
Hinges
Beam
1000 mm
1000 mm
Column
Pin Connections

(a)

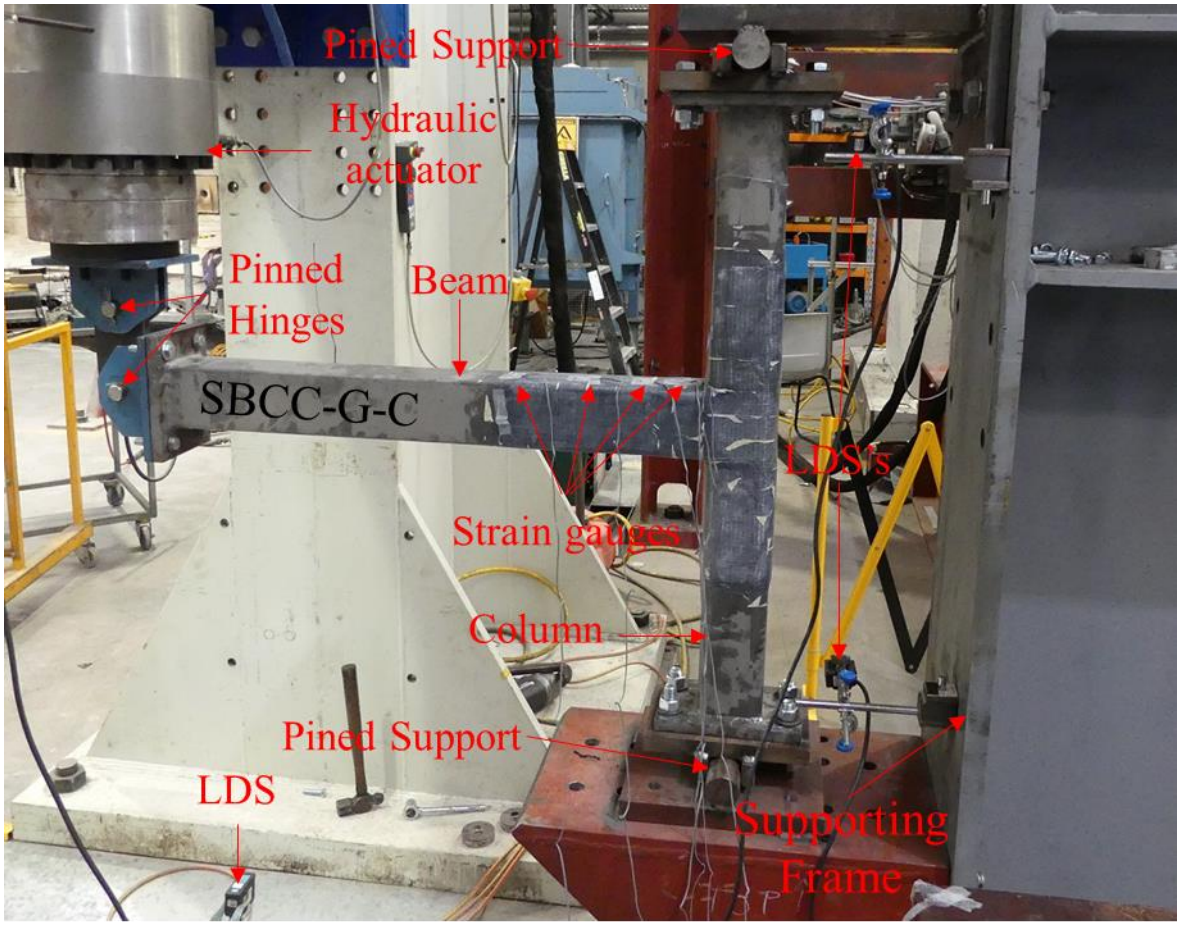

(b)

Figure 5: (a) Schematic diagram of the experimental setup (b) Photograph of the experimental setup

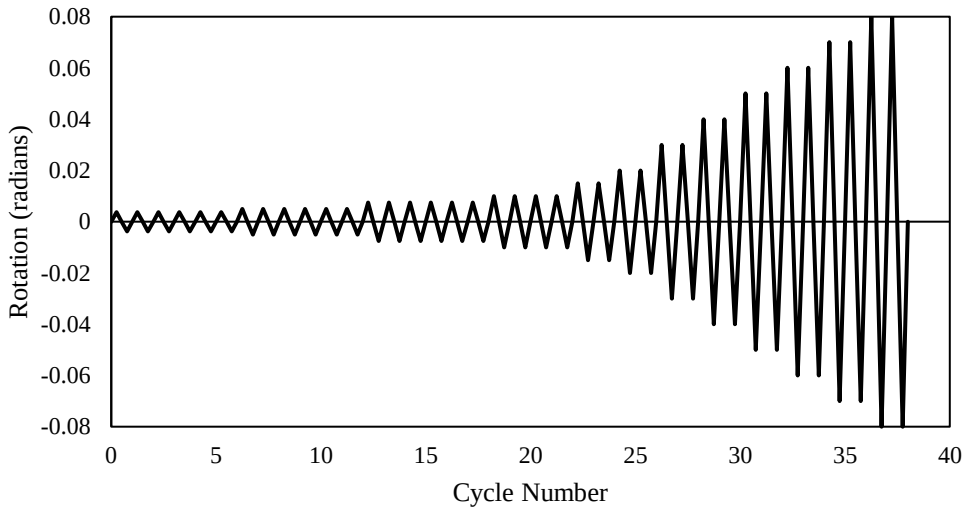

Figure 6: Cyclic loading protocol (adapted from [48])

3. Experimental Results and Discussion

Strengthening with CFRP and GFRP improves the structural response of the SHS beam-column connection. By aligning the longitudinal fibres of the sheets with the direction of loading and locking it in place with a transversely oriented hooping layer, the connections achieved greater ultimate moment capacity, secant stiffness, energy dissipation capacity and ductility.

3.1 Behaviour under monotonic loading

The bending response of bare, CFRP and GFRP strengthened connections under monotonic loading is evaluated and presented as moment-rotation curves. The applied load is multiplied by the lever arm of 1000 mm to calculate the moment capacity and plotted with the corresponding rotation for that moment. Moment capacity versus rotation curves of the bare, CFRP and GFRP strengthened SHS beam-column connections under monotonic loading are compared in Figure 7 which shows that the moment capacity is significantly increased for both CFRP and GFRP strengthened connections compared to the bare connection. The ultimate moment capacities of the bare, CFRP and GFRP strengthened SHS beam-column connections under monotonic loading are 19.1 kN.m, 25.6 kN.m and 25.5 kN.m respectively. The ultimate moment capacity of CFRP strengthened SHS connection is therefore improved by 34.2% while the GFRP strengthened SHS connection shows a slightly lower improvement of 33.8% compared to bare SHS connection under monotonic loading. Moreover, both CFRP and GFRP strengthened connections have been able to support higher rotational capacity of 0.042 radians and 0.053 radians respectively at the ultimate moment capacity compared to 0.028 radians of the bare connection. Moreover, Figure 8 exhibits the experimental failure modes of bare, CFRP and GFRP strengthened connections under monotonic loading where both of CFRP and GFRP strengthened connections are showed less buckling compared to bare connection. Fracture in weld was not observed during the testing. Moreover, the FRP strengthened connections failed

due to buckling of the steel beam under bending and fracture in the FRP was not observed during the experiments. Hence, the tensile strength of CFRP or GFRP was not the controlling factor, but their initial stiffness i.e. elastic modulus is the controlling factor. As the elastic modulus of the CFRP is higher than that of GFRP, CFRP strengthened connection showed higher moment capacity compared to the GFRP strengthened connection. On the other hand, GFRP strengthened connection shows a better rotational capacity compared to the CFRP strengthened connection due to its higher ductility property. However, sudden drops in the moment capacity occurred in both strengthened connections. These sudden drops may be due to some debonding on the compression sides, but the FRPs remained in their original positions since they were yet attached to the SHSs on the three other remaining sides. It can hence be concluded that both CFRP and GFRP strengthening techniques are effective to enhance the structural performance of SHS beam-column connections under monotonic loading.

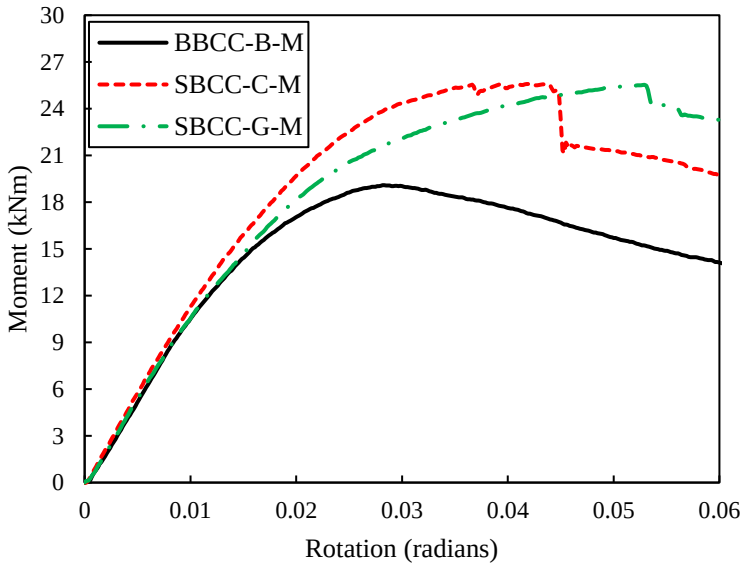

Figure 7: Moment-rotation curves of the bare, CFRP and GFRP strengthened connections under monotonic loading

(a) (b) (c)

Figure 8: Experimental failure modes of (a) bare, (b) CFRP and (c) GFRP strengthened connections under monotonic loading

The secant stiffness was determined by dividing the applied load by the corresponding displacement and plotted versus the rotation of the connections. The comparison of the secant stiffness curves of the bare, CFRP and GFRP strengthened SHS beam-column connections under monotonic loading is shown in Figure 9. The maximum secant stiffnesses of the CFRP and GFRP strengthened connections are 1156.3 kN/m and 1090.3 kN/m respectively which are 7.6% and 1.5% respectively higher compared to the maximum secant stiffness of 1074.4 kN/m of the bare connection. Secant stiffnesses for all connections are clearly seen to decrease with the increased rotation. At the ultimate deflection, the CFRP and GFRP strengthened connections have 39.6% and 64.9% greater secant stiffness compared to the that of the unstrengthened bare connection.

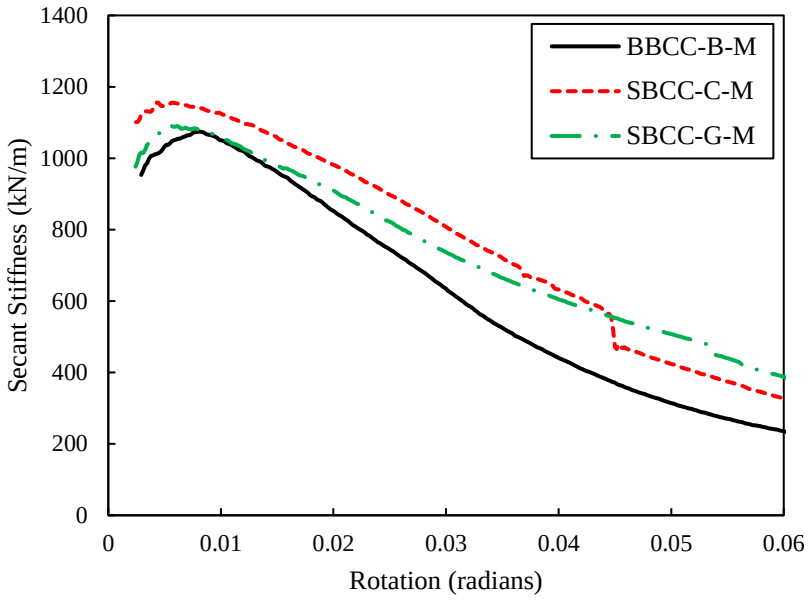

Figure 9: Secant stiffness-rotation curves of the bare, CFRP and GFRP strengthened connections under monotonic loading

The final performance factor under monotonic loading is the ductility factor for each connection. The ductility of connections in a steel frame has a significant effect on the structure's performance under seismic loading. The ductility factor is obtained by finding the ratio of energy dissipation at the ultimate load to the energy dissipation at the yield point [49]. The yield point is obtained according to Li et al. [50]. The ductility factors of all connections are shown in Figure 10. The improved ductility of both FRP reinforced connections over that of the bare steel connection is clear. The ductility factors of the bare, CFRP and GFRP strengthened SHS beam-column connections are 1.65, 2.03 and 2.50 respectively. Hence, due to the CFRP strengthening, the ductility of the SHS connections is increased by 22.9% and 51.4% due to the GFRP strengthening respectively. These increases in ductility factors are due to the increased post-yield capacities of the FRP wrapped connections.

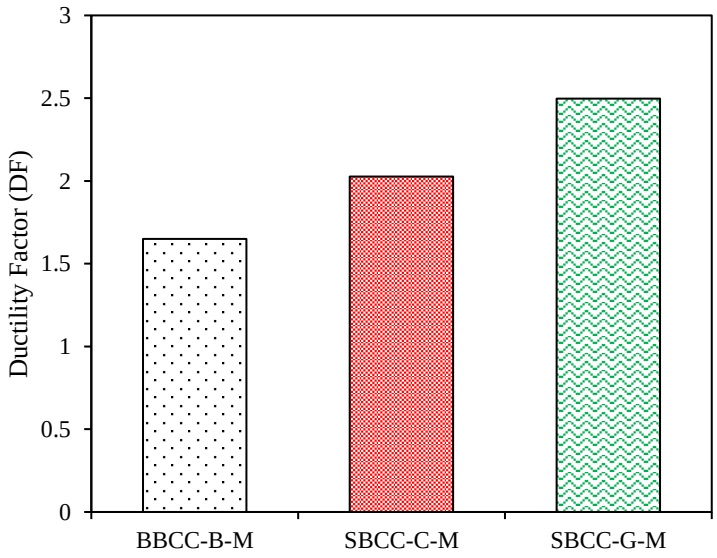

Figure 10: Ductility factors of the bare, CFRP and GFRP strengthened connections under monotonic loading

3.2 Behaviour under cyclic loading

Both CFRP and GFRP have been used to strengthen the welded steel SHS connections and tested alongside an identical bare connection. These tests are subjected to cyclic loads intended to simulate the cyclic effects of earthquake loading. The data from these tests have been analysed and plotted in terms of cyclic hysteretic responses, moment-rotation backbone curves, secant stiffnesses, energy dissipation capacities and plastic hinge development for clarity. These data and the summaries confirm the effectiveness of both FRP strengthening techniques. The sections below show the improvement of structural performances due to CFRP and GFRP strengthening over the bare connection under cyclic loading.

3.2.1 Experimental hysteretic behaviour

The cyclic bending responses of the bare, CFRP and GFRP strengthened SHS beam-column connections have been evaluated through hysteretic moment-rotation analysis. The moment capacity is calculated by multiplying the applied load by the lever arm of the loading point

(1000 mm) and plotted against the rotation measured in radians. Moment capacity versus rotation hysteresis responses of the bare, CFRP and GFRP strengthened SHS connections are shown in Figure 11(a), Figure 11(b) and Figure 11(c) respectively. Moreover, Figure 12 exhibits the experimental failure modes of bare, CFRP and GFRP strengthened connections under cyclic loading. All SHS connections behaved inelastically as seen from the hysteretic loops. Towards the end of the loading protocol specially after the yielding, a decrease in moment capacity is seen on the second cycle of each rotation level. This decrease was more significant in each of the subsequent higher rotation cycles. The moment capacity under cyclic loading has greatly improved in both CFRP and GFRP strengthened connections compared to that of the bare connection. For the positive rotation, the maximum moment capacity is 18.0 kN.m for the bare, 25.5 kN.m for the CFRP strengthened and 23.8 kN.m for the GFRP strengthened SHS beam-column connections. This shows that the CFRP strengthening increases the connection's maximum moment capacity by 41.3% and 31.8% respectively. Similarly, an increase in maximum moment capacities of both FRP strengthened connections are seen in the negative rotation. The maximum capacity for negative direction is 17.9 kN.m, 23.6 kN.m and 23.4 kN.m for the bare, CFRP and GFRP strengthened connections respectively. Hence, the maximum moment capacity in the negative rotation is slightly smaller than the maximum moment capacity in the positive rotation for each type of connection. Moreover, an increase in maximum moment capacity by 32.1% for the CFRP and 31.0% for GFRP strengthened connections over the bare specimen can be noticed in the negative rotation. Additionally, the bare, CFRP and GFRP strengthened connections reached the maximum moments at the rotational levels of 0.03 radian, 0.04 radian and 0.05 radian respectively in both positive and negative directions. Hence, both CFRP and GFRP strengthened connections reached higher rotational levels than the bare connection whereas GFPR strengthened connection reached a higher rotational level than the CFPR strengthened connection.

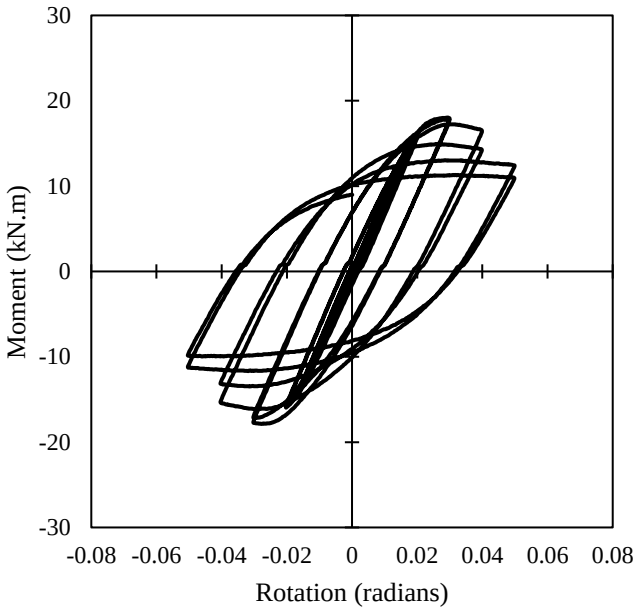
30
20
10
0
-10
-20
-30
Moment (kN.m)
-0.08 -0.06 -0.04 -0.02 0 0.02 0.04 0.06 0.08
Rotation (radians)

(a)

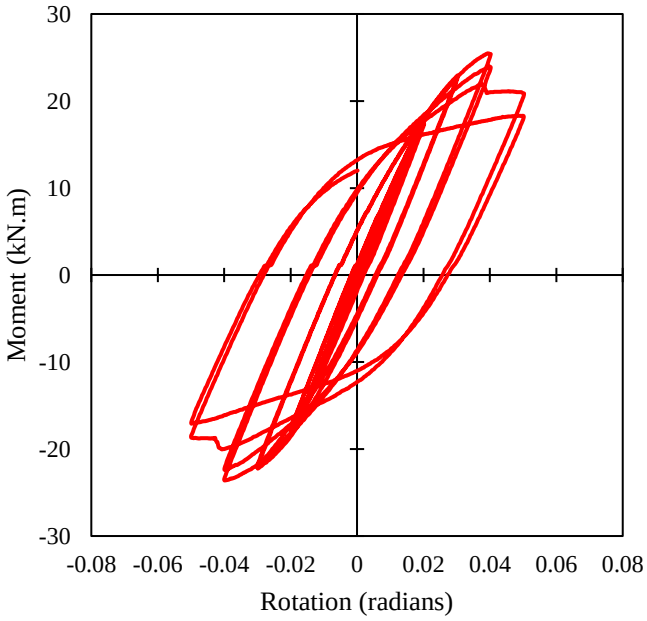
30
20
10
0
-10
-20
-30
Moment (kN.m)
-0.08 -0.06 -0.04 -0.02 0 0.02 0.04 0.06 0.08
Rotation (radians)

(b)

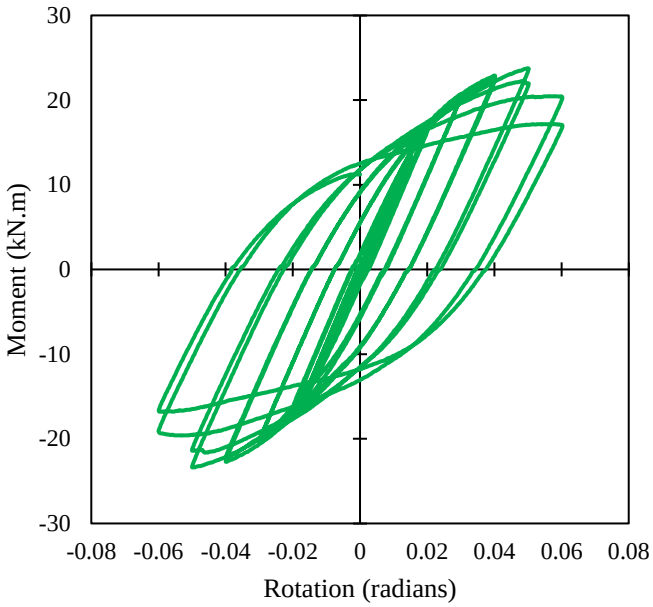

(c)

Figure 11: Moment capacity-rotation hysteresis curves of the (a) bare, (b) CFRP and (c) GFRP strengthened SHS connections

(a) (b) (c)

Figure 12: Experimental failure modes of (a) bare, (b) CFRP and (c) GFRP strengthened connections under cyclic loading

3.2.2 Moment Capacity Degradation Behaviour

Moment capacity degradation behaviour was analysed through moment versus rotation backbone curves for each tested connection. The backbone curves were created by plotting the moment at the maximum rotation of the first cycle of each rotation against the corresponding

maximum rotation. The moment versus rotation backbone curves of the bare, CFRP and GFRP strengthened SHS beam-column connections under cyclic loading are shown in Figure 13 which highlights the moment versus rotation hysteresis responses shown in Figure 11(a), (b) and (c). All connections show stable responses by exhibiting symmetric moment-rotation responses in both positive and negative directions. Moreover, all connections showed a decrease in moment capacity with each subsequent rotational level after reaching the ultimate moment (as rotations become larger). The decreasing moment capacity is due to local buckling in the beam connections of each specimen. Both FRP strengthened connections maintained higher moment capacities at the higher rotations and post-buckling, even at maximum rotation. In the positive direction, the bare connection has the maximum moment capacity of 18.0 kN.m at 0.03 radian rotation and reducing to 12.4 kN.m at the maximum rotation of 0.05 radians. The CFRP strengthened connection reached the maximum moment capacity of 25.5 kN.m at 0.04 radians and dropping to 20.9 kN.m at the maximum rotation of 0.05 radians. This shows a reduction of 31.1% in the moment capacity of the bare connection and 18.0% for the CFRP strengthened connection. On the other hand, GFRP strengthened connection did not show any moment degradation until the rotational level of 0.05 radians. Hence, the GFRP strengthened connection exhibits a better moment degradation behaviour than the CFRP strengthened connection and the CFRP strengthened connection exhibits a better moment degradation behaviour than the bare connection. Moreover, the GFRP strengthened connection reached the maximum moment capacity of 23.8 kN.m at 0.05 radians and dropping to 20.4 kN.m (14.3% reduction) at the rotation of 0.06 radians. In addition, after yielding the reduction in moment capacity occurred on each cycle within a given rotation level as well (can be seen from Figure 11). For the same rotation level, the bare, CRFP and GFRP strengthened connections moment capacities dropped by a maximum of 14.3 %, 13.4% and 16.3% between two cycles within a given rotation level.

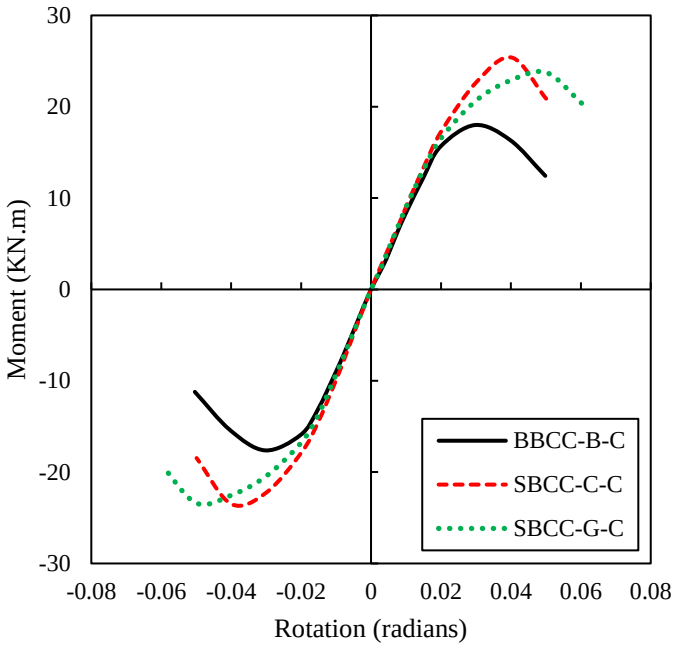

Figure 13: Moment capacity-rotation hysteresis backbone curves of the bare, CFRP and GFRP strengthened SHS connections.

3.2.3 Secant Stiffness

Secant stiffness for each rotational level is calculated through dividing the applied load (at maximum displacement) by the maximum displacement of that particular rotation. The calculated secant stiffness is then plotted against the corresponding rotation in radians for each connection type. Secant stiffness-rotation curves for bare, CFRP and GFRP strengthened SHS beam-column connections are compared in Figure 14. It can be seen that as the rotation increases with each loading cycle, the secant stiffness for all connections decreased. For the positive rotation, the bare, CFRP and GFRP strengthened connections have maximum secant stiffnesses of 838.4 kN/m, 901.4 kN/m and 898.9 kN/m respectively at 0.01 radians. This results in 7.5% and 7.2% improvements in secant stiffness due to CFRP and GFRP strengthening. Although all connections lost stiffness gradually, the bare steel section suffered a greater stiffness degradation compared to FRP strengthened connections. The bare section lost 70.2% stiffness at 0.05 radians while the CFRP and GFRP strengthened connections lost

53.7% and 47.3% respectively of their stiffness at 0.05 radians. Hence, the stiffness of CFRP and GFRP have a significant effect on the strengthening of SHS connections. The CFRP strengthened connection showed a higher stiffness due to the higher stiffness characteristics of CFRP compared to GFRP whereas the GFRP strengthened connection showed less degradation of stiffness due to the high ductility characteristics of GFRP compared to CFRP. Moreover, at the final rotation of bare connection (0.05 radians), the CFRP and GFRP strengthened connections have 67.1% and 89.9% respectively higher secant stiffness compared to the bare connection. At the ultimate moment capacity point of bare connection (0.03 radians), the secant stiffnesses of the CFRP and GFRP strengthened connections are 24.3% and 13.5% respectively higher than the bare connection.

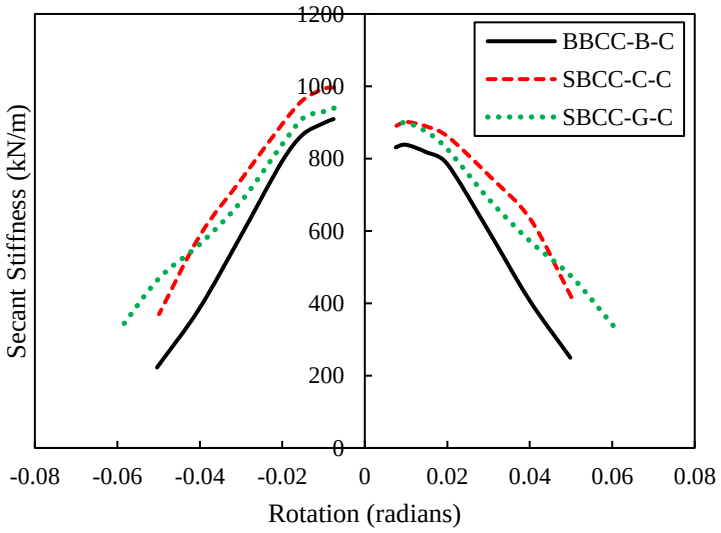

Figure 14: Secant stiffness-rotation curves of the bare, CFRP and GFRP strengthened SHS connections

3.2.4 Energy Dissipation Capacity

The effects of CFRP and GFRP strengthening on energy dissipation capacity under cyclic loading are investigated. Seismic energy is mostly dissipated through specific elements that deform inelastically in a structure. The base of columns, beams and intermediate panels will

generally inelastically deform to dissipate energy in the steel-framed buildings. Therefore, the capacities of strengthened and bare connections have for energy dissipation are critical when considering earthquake input energy. The energy dissipation capacity is determined by calculating the area enclosed by all cycles of each rotation level and plotted against the rotation. The energy dissipation capacity versus rotation curves of bare, CFRP and GFRP strengthened connections are shown in Figure 15. The dissipated energy for each specimen remained low in the elastic region (almost until the rotation of 0.02 radians). These increased rapidly for all connections after yielding, with that for the bare connection increasing slightly faster than those for the FRP wrapped connections. At the ultimate moment capacity point of each connection, the bare connection has dissipated 1.01 kN.m of energy, while the CFRP strengthened dissipated 1.86 kN.m, an increase of 84.2% and the GFRP strengthened dissipated 3.06 kN.m, an increase of 203.9%. The increased maximum moment capacity and rotational capacity allow the CFRP and GFRP connections to dissipate more energy as they can handle much higher loads and rotations before failure. Moreover, at the rotation of 0.05 radian, CFRP and GFRP strengthened connections have shown higher energy dissipation capacities of 24.54% and 16.2% respectively compared to the bare connection.

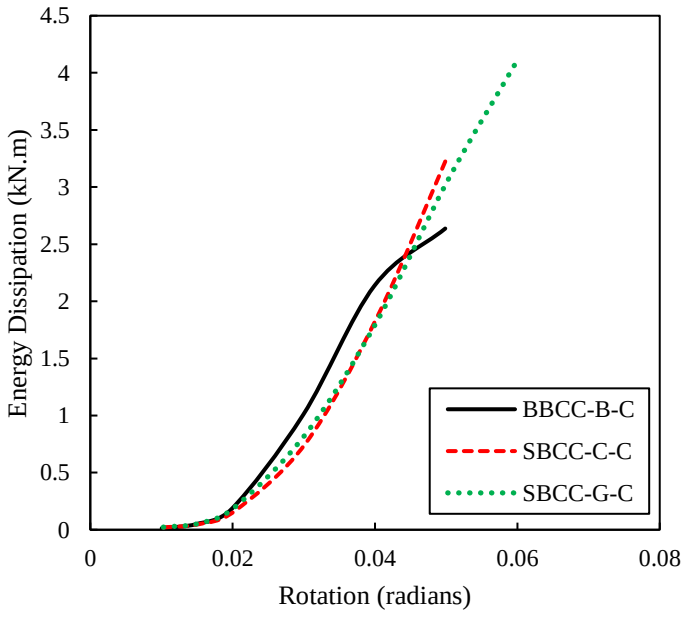

Figure 15: Energy dissipation-rotation curves of the bare, CFRP and GFRP strengthened SHS connections

3.2.5 Plastic Hinge Development

The development of plastic hinges in the bare and FRP strengthened SHS connections are also discussed and compared to investigate the effectiveness of both FRP strengthening techniques. The propagation of yielding along the beam length was investigated through the distribution characteristics of strain along the beam length. The strain distribution along the beam length was measured by four strain gauges placed at 50 mm, 100 mm, 200 mm and 300 mm distances from the column front face at the centre of the top face of the beam. The value of the yield strain of steel is 2000 (με) and was calculated based on the steel yield stress of steel. The strains of bare, CFRP and GFRP strengthened SHS beam-column connections are compared at the rotation levels of 0.01 radian, 0.03 radian, 0.04 radian and 0.05 radian which represent small, medium, high and very high levels of rotation respectively. The comparison of the strains at different rotational levels of the bare, CFRP and GFRP strengthened connections are shown in Figure 16, Figure 17 and Figure 18 respectively.

At the rotational level of 0.01 radian, the bare SHS beam remains elastic in both tension and compression. At the rotational level of 0.03 radian, yielding has spread as a minimum of 200 mm of the bare SHS beam from the connection. However, at the rotational level of 0.04 and 0.05 radians, reductions in the strains of bare SHS beam are found at 50 mm, 100 mm, 200 mm and 300 mm from the column end (compared to that at the rotation of 0.03 radian). Hence, local buckling occurred in the bare SHS beam before the rotational level of 0.04 radian and at less than 50 mm from the connection. On the other hand, the strains in the CFRP and GFRP strengthened SHS beams increased up to the rotation of 0.04 and 0.05 radians. Then reductions in strains occur at all gauges compared to those at the previous rotation of 0.04 radian in the CFRP strengthened beam and 0.05 radian in the GFRP strengthened beam. Hence, FRP

strengthening technique can effectively enhance the SHS beam rotational capacity and the local buckling has been delayed as a result of CFRP and GFRP strengthening from 0.04 radian to 0.05 radian and 0.04 radian to 0.06 radian respectively.

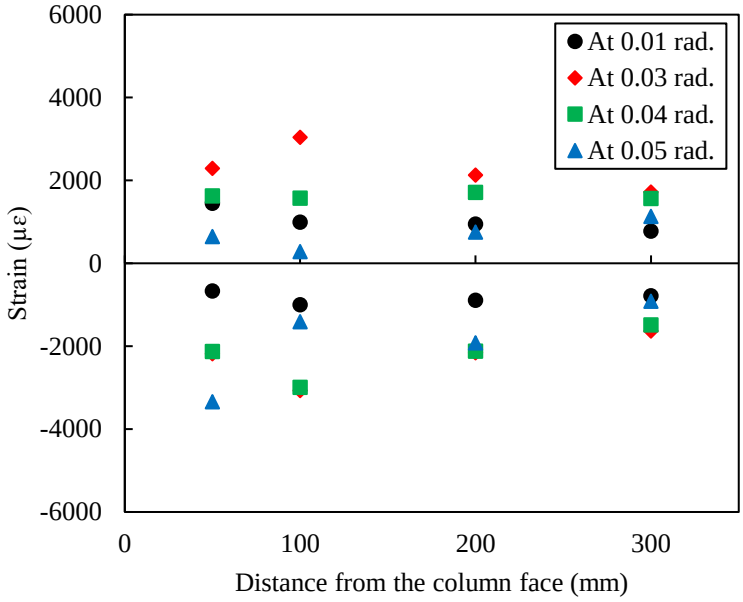

Figure 16: Strain distribution along the beam length of the bare connection

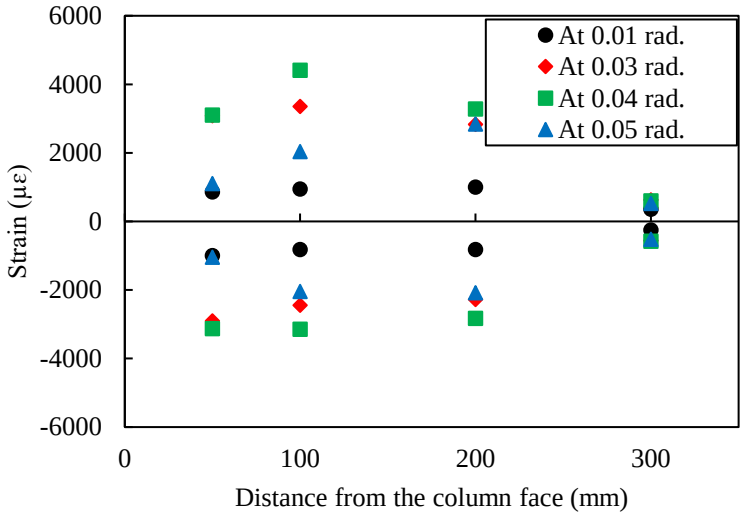

Figure 17: Strain distribution along the beam length of the CFRP Strengthened connection

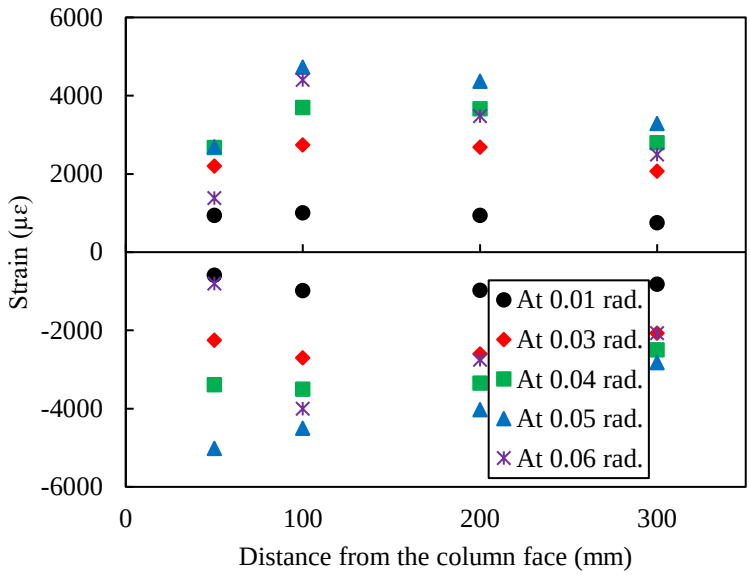

Figure 18: Strain distribution along the beam length of the GFRP Strengthened connection

4. Conclusions

Experimental investigations have been conducted on the behaviour of bare, CFRP and GFRP strengthened SHS connections under both monotonic and cyclic loadings. Both CFRP and GFRP strengthening techniques are found to have enhanced the structural performances effectively under both monotonic and cyclic loadings. The major benefits and conclusions of CFRP and GFRP strengthening technique are outlined as follow:

1. Both CFRP and GFRP strengthening techniques are effective for enhancing the ultimate moment capacity and rotational capacity of SHS beam-column connections under monotonic loading where the CFRP strengthened connection shows a slightly higher ultimate moment capacity while the GFRP strengthened connection shows better rotational capacity.
2. Although the stiffness and ductility of SHS beam-column connections can be effectively enhanced under monotonic loading by both CFRP and GFRP strengthening, the CFRP strengthened connection exhibited better performance in terms of secant stiffness due to

its higher ultimate moment capacity whereas the GFRP strengthened connection exhibited better performance in terms of ductility due to its higher rotational capacity.

3. The CFRP and GFRP strengthening techniques improved the maximum moment capacity of the SHS beam-column connection by 41.3% and 31.8% respectively under cyclic loading. Additionally, both CFRP and GFPR strengthened connections reached maximum moment capacities at the higher rotational levels of 0.04 and 0.05 radian respectively compared to the bare connection which reached its maximum moment capacity at 0.03 radian.
4. Both CFRP and GFRP strengthened SHS connections exhibited more stable hysteresis responses by showing less moment degradation behaviour compared to bare SHS connection. GFRP strengthened SHS connections showed less moment degradation compared to CFRP strengthened SHS connections due to the higher ductility characteristics of GFRP compared to CFRP.
5. The stiffness of CFRP and GFRP have a significant effect on the strengthening of the SHS connections under cyclic loading. The CFRP strengthened connection showed higher stiffness due to the higher stiffness characteristics of CFRP compared to GFRP, whereas the GFRP strengthened connection showed less degradation of stiffness as the GFRP strengthened connection showed less moment degradation compared to the CFRP strengthened connection.
6. The increased maximum moment capacity and rotational capacity allow the CFRP and GFRP connections to dissipate more energy under cyclic loading. The energy dissipation capacity of SHS connection was enhanced by 84.2% and 203.9% as a result of CFRP and GFRP strengthening respectively under cyclic loading at the ultimate moment capacity point of each connection.

7. FRP strengthening technique can effectively enhance the SHS beam rotational capacity under cyclic loading where the local buckling is delayed from 0.04 radian to 0.05 radian and 0.04 radian to 0.06 radian as a result of CFRP and GFRP strengthening respectively.

Acknowledgment

The authors would wish to thank the technical staff of the Banyo Pilot Plant Precinct of Queensland University of Technology (QUT), Mr. Frank De Bruyne, Mr. Barry Hume and Mr. Cameron Creevey, for their technical support to conduct the reported experimental testing. The authors also would wish to thank the School of Civil and Environmental Engineering of Queensland University of Technology (QUT), Australia for the financial support to conduct the reported experimental testing.

Data Availability Statement

Sharing of the raw data of the present research is not possible at this stage as the outcomes of the present research are a part of an ongoing study.

Reference

[1] Wardenier J, Packer JA, Zhao XL, Van der Vegte GJ. Hollow sections in structural applications. Bouwen met Staal Rotterdam,, The Netherlands; 2002.

[2] Tafsirojjaman T, Fawzia S, Thambiratnam D, Zhao X. Numerical investigation of CFRP strengthened RHS members under cyclic loading. Structures 2020;24:610–26. https://doi.org/10.1016/j.istruc.2020.01.041.

[3] Guha-Sapir D, Below R, Hoyois P. EM-DAT: International disaster database. Cathol Univ Louvain Brussels, Belgium 2015.

[4] Nazri FM. Prediction of The Collapse Load for Moment-Resisting Steel Frame Structure Under Earthquake Forces (Penerbit USM). Penerbit USM; 2015.

[5] Seica M V., Packer JA. FRP materials for the rehabilitation of tubular steel structures, for underwater applications. Compos Struct 2007;80:440–50. https://doi.org/10.1016/j.compstruct.2006.05.029.

[6] Kaan BN, Alemdar F, Bennett CR, Matamoros A, Barrett-Gonzalez R, Rolfe S. Fatigue enhancement of welded details in steel bridges using CFRP overlay elements. J Compos Constr 2012;16:138–49. https://doi.org/10.1061/(ASCE)CC.1943-5614.0000249.

[7] Alemdar F, Matamoros A, Bennett C, Barrett-Gonzalez R, Rolfe ST. Use of CFRP overlays to strengthen welded connections under fatigue loading. J Bridg Eng 2012;17:420–31. https://doi.org/10.1061/(ASCE)BE.1943-5592.0000230.

[8] Mahin S a. Lessons from damage to steel buildings during the Northridge earthquake. Eng Struct 1998;20:261–70. https://doi.org/10.1016/S0141-0296(97)00032-1.

[9] Youssef NFG, Bonowitz D, Gross JL. A survey of steel moment-resisting frame buildings affected by the 1994 Northridge earthquake. US National Institute of Standards and Technology; 1995.

[10] Nakashima M, Inoue K, Tada M. Classification of damage to steel buildings observed in the 1995 Hyogoken-Nanbu earthquake. Eng Struct 1998;20:271–81. https://doi.org/10.1016/S0141-0296(97)00019-9.

[11] Tafsirojjaman T, Fawzia S, Thambiratnam D, Zhao XL. Seismic strengthening of rigid steel frame with CFRP. Arch Civ Mech Eng 2019;19:334–47. https://doi.org/10.1016/j.acme.2018.08.007.

[12] Tafsirojjaman, Fawzia S, Thambiratnam D. Enhancement Of Seismic Performance Of Steel Frame Through CFRP Strengthening. Procedia Manuf 2019;30:239–46. https://doi.org/10.1016/j.promfg.2019.02.035.

[13] Chandrathilaka ERK, Gamage JCPH, Fawzia S. Mechanical characterization of CFRP/steel bond cured and tested at elevated temperature. Compos Struct 2019;207:471–7. https://doi.org/10.1016/j.compstruct.2018.09.048.

[14] Batuwitage C, Fawzia S, Thambiratnam DP, Tafsirojjaman T, Al-Mahaidi R, Elchalakani M. CFRP-wrapped hollow steel tubes under axial impact loading. Tubul. Struct. XVI Proc. 16th Int. Symp. Tubul. Struct. (ISTS 2017, 4-6 December 2017, Melbourne, Aust., CRC Press; 2017, p. 401.

[15] Liu Y, Tafsirojjaman T, Dogar AUR, Hückler A. Bond behaviour improvement between infra-lightweight and high strength concretes using FRP grid reinforcements and development of bond strength prediction models. Constr Build Mater 2020;270:121426. https://doi.org/10.1016/j.conbuildmat.2020.121426.

[16] Tafsirojjaman T, Fawzia S, Thambiratnam DP, Zhao XL. Study on the cyclic bending behaviour of CFRP strengthened full-scale CHS members. Structures 2020;28:741–56. https://doi.org/10.1016/j.istruc.2020.09.015.

[17] Liu Y, Tafsirojjaman T, Dogar AUR, Hückler A. Shrinkage behavior enhancement of infra-lightweight concrete through FRP grid reinforcement and development of their shrinkage prediction models. Constr Build Mater 2020;258.

[18] Teng JG, Chen JF, Smith ST, Lam L. Behaviour and strength of FRP-strengthened RC structures: a state-of-the-art review. Proc Inst Civ Eng - Struct Build 2003;156:51–62. https://doi.org/10.1680/stbu.2003.156.1.51.

[19] Tafsirojjaman T, Fawzia S, Thambiratnam D, Zhao XL. Behaviour of CFRP strengthened CHS members under monotonic and cyclic loading. Compos Struct 2019;220:592–601. https://doi.org/10.1016/j.compstruct.2019.04.029.

[20] Tafsirojjaman T, Fawzia S, Thambiratnam DP. Investigation on the behaviour of CFRP strengthened CHS members under Monotonic loading through finite element modelling. Structures 2020;28:297–308.

[21] Alam MI, Fawzia S, Tafsirojjaman T, Zhao XL. FE modeling of FRP strengthened CHS members subjected to lateral impact. Tubul. Struct. XVI Proc. 16th Int. Symp. Tubul. Struct. (ISTS 2017, 4-6 December 2017, Melbourne, Aust., CRC Press; 2017, p. 409.

[22] Tafsirojjaman T, Fawzia S, Thambiratnam D. Numerical investigation on the CFRP strengthened steel frame under earthquake. Mater. Sci. Forum Front. Compos. Mater. IV, Trans Tech Publications Ltd.; 2019.

[23] Tafsirojjaman T, Fawzia S, Thambiratnam D. Numerical investigation on the seismic strengthening of steel frame by using normal and high modulus CFRP. Proc. seventh Asia-Pacific Conf. FRP Struct., International Institute for FRP in Construction (IIFC); 2019.

[24] Siddique MAA, El Damatty AA, El Ansary AM. A numerical investigation of overstrength and ductility factors of moment resisting steel frames retrofitted with GFRP plates. Can J Civ Eng 2014;41:17–31. https://doi.org/10.1139/cjce-2012-0271.

[25] Siddique MAA, El Damatty AA. Improvement of local buckling behaviour of steel beams through bonding GFRP plates. Compos Struct 2013;96:44–56. https://doi.org/10.1016/j.compstruct.2012.08.042.

[26] Accord NB, Earls CJ. Use of Fiber-Reinforced Polymer Composite Elements to Enhance Structural Steel Member Ductility. J Compos Constr 2006;10:337–44. https://doi.org/10.1061/(ASCE)1090-0268(2006)10:4(337).

[27] Hu L, Feng P, Zhao XL. Fatigue design of CFRP strengthened steel members. Thin-

Walled Struct 2017;119:482–98. https://doi.org/10.1016/j.tws.2017.06.029.

[28] Liu H, Xiao Z, Zhao XL, Al-Mahaidi R. Prediction of fatigue life for CFRP-strengthened steel plates. Thin-Walled Struct 2009;47:1069–77. https://doi.org/10.1016/j.tws.2008.10.011.

[29] Feng P, Hu L, Zhao XL, Cheng L, Xu S. Study on thermal effects on fatigue behavior of cracked steel plates strengthened by CFRP sheets. Thin-Walled Struct 2014;82:311–20. https://doi.org/10.1016/j.tws.2014.04.015.

[30] Bambach MR, Jama HH, Elchalakani M. Axial capacity and design of thin-walled steel SHS strengthened with CFRP. Thin-Walled Struct 2009;47:1112–21. https://doi.org/10.1016/j.tws.2008.10.006.

[31] Bambach MR, Elchalakani M. Plastic mechanism analysis of steel SHS strengthened with CFRP under large axial deformation. Thin-Walled Struct 2007;45:159–70. https://doi.org/10.1016/j.tws.2007.02.004.

[32] Kalavagunta S, Naganathan S, Bin Mustapha KN. Proposal for design rules of axially loaded CFRP strengthened cold formed lipped channel steel sections. Thin-Walled Struct 2013;72:14–9. https://doi.org/10.1016/j.tws.2013.06.006.

[33] Ganesh Prabhu G, Sundarraja MC, Kim YY. Compressive behavior of circular CFST columns externally reinforced using CFRp composites. Thin-Walled Struct 2015;87:139–48. https://doi.org/10.1016/j.tws.2014.11.005.

[34] Kurobane Y, Packer JA, Wardenier J, Yeomans N. Design Guide for Structural Hollow Section Column Connections. 2004.

[35] Wang M, Shi Y, Wang Y, Shi G. Numerical study on seismic behaviors of steel frame end-plate connections. J Constr Steel Res 2013;90:140–52.

https://doi.org/10.1016/j.jcsr.2013.07.033.

[36] Wu C, Zhao XL, Al-Mahaidi R, Emdad MR, Duan WH. Fatigue tests on steel plates with longitudinal weld attachment strengthened by ultra high modulus carbon fibre reinforced polymer plate. Fatigue Fract Eng Mater Struct 2013;36:1027–38. https://doi.org/10.1111/ffe.12067.

[37] Mashiri FR, Zhao XL. Fatigue tests and design of welded thin-walled RHS-RHS and RHS-angle cross-beam connections under cyclic bending. Thin-Walled Struct 2010;48:159–68. https://doi.org/10.1016/j.tws.2009.07.006.

[38] Nakamura H, Jiang W, Suzuki H, Maeda, Irube T. Experimental study on repair of fatigue cracks at welded web gusset joint using CFRP strips. Thin-Walled Struct 2009;47:1059–68. https://doi.org/10.1016/j.tws.2008.10.016.

[39] Tong L, Xu G, Zhao X-L, Zhou H, Xu F. Experimental and theoretical studies on reducing hot spot stress on CHS gap K-joints with CFRP strengthening. Eng Struct 2019;201:109827.

[40] AS/NZS 1163. Cold-formed structural steel hollow sections, Standards Australia., 2016.

[41] AS 1391. Metallic materials-Tensile testing at ambient temperature, 2007.

[42] ASTM D3039. Standard Test Method for Tensile Properties of Polymer Matrix Composite Materials, 2008.

[43] Alam MI, Fawzia S, Zhao XL, Remennikov AM, Bambach MR, Elchalakani M. Performance and dynamic behaviour of FRP strengthened CFST members subjected to lateral impact. Eng Struct 2017;147:160–76. https://doi.org/10.1016/j.engstruct.2017.05.052.

[44] Kabir MH, Fawzia S, Chan THT, Gamage JCPH, Bai JB. Experimental and numerical

investigation of the behaviour of CFRP strengthened CHS beams subjected to bending. Eng Struct 2016;113:160–73. https://doi.org/10.1016/j.engstruct.2016.01.047.

[45] ASTM D638. Standard Test Method for Tensile Properties of Plastics., 2010.

[46] Kabir MH, Fawzia S, Chan THT, Badawi M. Durability of CFRP strengthened steel circular hollow section member exposed to sea water. Constr Build Mater 2016;118:216–25. https://doi.org/10.1016/j.conbuildmat.2016.04.087.

[47] ANSI/AWS D1.1. Structural Welding-Steel, American Welding Society. American Welding Society; 2010.

[48] ANSI/AISC 341-16. Seismic Provisions for Structural Steel Buildings, 2016. https://doi.org/111.

[49] Duarte APC, Silva BA, Silvestre N, de Brito J, Júlio E, Castro JM. Tests and design of short steel tubes filled with rubberised concrete. Eng Struct 2016;112:274–86. https://doi.org/10.1016/j.engstruct.2016.01.018.

[50] Li ZX. Theory and technique of engineering structure experiments. Tianjin Univ Press Tianjin 2004.